12-18-1995

Application Of An Optical Remote Sensing Model

Charles Bostater

Wei-ming Ma

Ted McNally

Manuel Gimond

A. P. Lamb

PROCEEDINGS OF SPIE

SPIEDigitalLibrary.org/conference-proceedings-of-spie

Application of an optical remote sensing model

Charles R. Bostater
Wei-ming Ma
Ted McNally
Manuel Gimond
A. P. Lamb

SPIE.

Application of an optical remote sensing model

Charles Bostater, Wei-ming Ma, Ted McNally, Manuel Gimond, and A. P. Lamb

Marine & Environmental Optics Laboratory, Center for Remote Sensing
Marine & Environmental Systems Division
Florida Institute of Technology
150 West University Blvd.
Melbourne FL., 32901

ABSTRACT

A simplified two-flow model derived from the radiative transfer problem applicable to a water column is described and applied. The application of the model to reflectance signatures measured in Delaware Bay estuarine waters is described. The shapes of the reflectance signatures compare nicely with field data, although the absolute magnitudes of reflectance are different. The model could be improved if a more realistic non-homogeneous model is applied or actual absorption coefficients were measured. An analytic two-flow model was developed and the sensitivity analysis runs for estimating radiance reflectance (nadir view geometry) above the water surface suggest that the most important in-situ parameters are absorption coefficient, the internal diffuse reflectance coefficient, and the backscatter coefficient.
Keywords: absorption, backscattering, reflectance, bottom reflectance, model, radiance, irradiance.

1. INTRODUCTION

The incident solar irradiance in the visible wavelength range at the sea surface has a significant influence on physical and biological processes in the ocean. Knowledge of the radiance distribution in the ocean is important information necessary for solutions to more specific problems and studies of photosynthesis, water depth, and bottom types in coastal ocean waters. The fundamental parameters of interest in remote sensing of coastal waters types are the water surface reflectance, and the attenuation, absorption, and backscatter of electromagnetic energy[1]. The irradiance reflectance of shallow water, which is derived from a two-flow model of the underwater light field, is a function of the water depth, water optical properties, and bottom reflectance. The reflectance can be used for measuring primary production, dissolved organic matter, suspended matter (i.e. water quality constituents), bottom types, and water depth in the estuarine and coastal ocean waters.

Remote sensing in shallow water environments presents a special problem to those interested in gathering spectral reflectance data about such areas. Once the water column becomes optically shallow, the irradiance reflectance spectra at the surface is now influenced by the bottom reflectance signatures. As the bottom influence increases, one must become increasingly concerned with accurately modeling and accounting for this factor. One might ask "How much does the bottom reflectance contribute to the measured reflectance just above or below the surface as a function of wavelength?". Before inverting a model for estimation of water quality parameters, one must begin to quantitatively determine the influence of the bottom on reflectance. To quantitatively determine the influence of the bottom on reflectance, one needs to know about the absorbance and backscatter of at least a homogeneous water column above the bottom, the water depth, and bottom reflectance signature as we will demonstrate in this paper.

A description of an analytical two-flow model is derived and applied in this paper. The model describes the change of irradiance per unit depth along the vertical direction for a horizontally homogeneous medium or the light field in the ocean. The loss of upwelling and downwelling irradiance in the model is assumed to be due to the absorption and backscattering of the irradiance due to water, phytoplankton chlorophyll, dissolved organic matter, and suspended matter in the water. The gain of upwelling and downwelling irradiance is assumed to be also due to scattering (conversion) of

0-8194-1950-8/95/$6.00

specular flux density for the Case II model described below. A mathematical solution to the simplified two-flow equations exists when the equations are decoupled into a set of second order non-homogeneous differential equations as shown by Bostater et al[2]. The model proposed for application will use boundary condition formulations applicable to a flat ocean surface. The results of a sensitivity analysis are presented for the explicit solution to the two-flow equations.

2. BACKGROUND

The propagation of light in the ocean-atmosphere system is governed by the integral-differential equation of radiative transfer, which contains absorption and scattering parameters that are characteristic of the particular water body under study. Because the radiance is very difficult to measure, most light field measurements involve integrals of the radiance distribution. The integration of the radiance equation produces the equations describing upwelling and downwelling irradiance.

Although several deterministic mathematical models[3] have been developed to characterize the radiative transfer in stratified waters, the two-flow models of light fields are applicable in homogeneous optically shallow waters[4]. The two-flow models can contain upwelling and downwelling irradiance as well as a specular flux term based on radiative energy conservation. The two-flow model is solved analytically with unique boundary and initial conditions. The major advantage of the analytical model described here is its apparent simplicity, although several assumptions have been made to simplify the problem in order to obtain an analytical solution.

The approach we describe here is summarized as follows: (1) The two-flow model in the light field is derived and solved analytically; (2) The distribution of irradiance in typical coastal ocean water is simulated by using measured data; (3) The two-flow model of the light field is developed from integration of the radiative transfer equation over the downwelling and upwelling hemispheres; (4) The coupled two-flow model is decoupled into two second order homogeneous (Case I) or non-homogeneous differential equations (Case II) of downwelling and upwelling irradiance and one first order equation describing specular irradiance; (5) The coefficients of the general solutions are solved by Cramer's rule for the upper and bottom boundary conditions[2]; (6) The absorption, backscattering, attenuation, and conversion coefficients are adopted from the literature or obtained from field measurements; (7) The sensitivity of the reflectance to all the input parameters is calculted to find out the most sensitive parameters for future field measurements; (8) The reflectance signatures from the model are compared to measured data; (9) The influence of water quality variables and bottom reflectance is simulated in the reflectance signatures derived from the solutions.

3. THEORY

The two-flow model is derived from the radiative transfer equation (RTE). The RTE describes the change of radiance per unit depth dz along direction (θ, ϕ) for a horizontally stratified medium. If there are no internal sources of energy then the RTE is given by[1]:

$$\cos\theta \frac{dL(\theta,\phi;z)}{dz} = -c(z)L(\theta,\phi;z) + \int_0^{2\pi}\int_0^{\pi}\beta(\theta',\theta,\phi',\phi;z)L(\theta',\phi';z)\sin\theta' d\theta' d\phi + \beta(\theta_c,\theta,\phi_c,\phi;z)L_c(\theta_c,\phi_c;z). \quad (1)$$

where c(z) is the beam attenuation with units m^{-1}, $\beta(\theta',\theta,\phi',\phi;z)$ is the volume scattering function with units m^{-1} str^{-1} and shows how much of the radiance originally traveling in the direction (θ', ϕ') is scattered into the direction (θ, ϕ), $L(\theta',\phi';z)$ is the radiance with units W m^{-2} str^{-1}, and $L_c(\theta_c,\phi_c;z)$ is the scattered collimated radiance, with the subscript c representing collimated, with units W m^{-2} str^{-1}. The first term on the right-hand side of the radiative transfer equation is the loss of radiant energy from the radiance $L(\theta',\phi';z)$ due to absorption and scattering. The second and the third terms are the path radiance. These terms are the gain of radiant energy into the radiance $L(\theta,\phi;z)$ due to scattering of radiance energy initially traveling in the other direction (θ', ϕ') into the direction θ , ϕ in 3-D space[4].

The light field used in this research refers to radiation in the part of the electromagnetic spectrum from about 368 to 1110 nm. This region contains the portion of the electromagnetic spectrum within which plants conduct photosynthesis, namely 400 to 700 nm. All the optical parameters defined in this study are wavelength dependent. The wavelength is therefore not directly delineated in the nomenclature and definitions of optical parameters.

4. DEVELOPMENT OF TWO-FLOW MODEL

Two cases of the two-flow model are integrated using from the original RTE with or without the specular radiance, $L_C(\theta,\phi;z)$. Energy propagating in a downward direction is considered to be propagating in a positive, +z direction. Two common methods can be used to solve the two-flow equations. These include the use of matrix methods[4] and the classical algebraic method[2]. It is more appropriate to use the standard 2nd order ODE method as the solutions are more readily visualized and readily understood. We utilize here unique boundary conditions that allow an explicit solution of the resulting coupled 2nd order differential equations.

The following is a summary of the simplifying assumptions made in order to facilitate the solution and interpretation of the model as presented in this paper. These assumptions include:

(1). The optical absorption and backscatter coefficients are assumed constant with variable water column depth.

(2). The optical absorption and backscatter coefficients are assumed to be the constant for both the upward and downward directions.

(3). All irradiance once having entered the medium (water) is assumed to be independent of the angular distribution due to the effects of scattering.

(4). Only one coefficient is used for the conversion of specular irradiance, $E_S^W(z)$, into upwelling irradiance, $E_u^W(z)$, and downwelling irradiance, $E_u^W(z)$ in the non-homogeneous case (Case II).

(5). The water surface is assumed to be a perfectly flat horizontal plane.

4.1. Case I: The homogeneous two-flow model equations without specular radiance derived from Equation (1) are:

$$\frac{dE_d^w(z)}{dz} = -(a+b)E_d^w(z) + bE_u^w(z). \tag{2}$$

$$\frac{dE_u^w(z)}{dz} = (a+b)E_u^w(z) - bE_d^w(z). \tag{3}$$

where a is absorption and b is backscattering coefficients both with units m^{-1}. This model describes the changes of irradiance per unit depth along the vertical direction for a horizontally stratified or homogeneous medium. The loss of upwelling and downwelling irradiance is due to attenuation (absorption, a, and backscattering, b) by water, phytoplankton chlorophyll, dissolved substances, and suspended matter. Equations (2) and (3) are coupled in terms of $E_d^W(z)$ and $E_u^W(z)$. To solve for $E_d^W(z)$ and $E_u^W(z)$, a method of substitution of these variables is utilized to decouple these first order equations into two second homogeneous differential equations. The decoupled second order homogeneous irradiance equations are given as follows:

$$\frac{d^2E_d^w(z)}{dz^2} - (a^2+2ab)E_d^w(z) = 0 \tag{4}$$

$$\frac{d^2E_u^w(z)}{dz^2} - (a^2+2ab)E_u^w(z) = 0 \tag{5}$$

The objective of the two-flow problem is to predict upwelling irradiance, $E_u^W(0)$, at the surface. For the case of optically shallow waters (described in this paper), it cannot be assumed that z tends towards infinity. The bottom boundary condition in this case is the actual water depth (z = h) where h is the depth of the water column from the air-water interface to the bottom. Equations (4) and (5) are solved by using ODE methods to obtain general solutions. The coefficients of the general solution are of course determined by the appropriate boundary conditions. The boundary conditions and initial conditions used are[2]:

(1) The downwelling irradiance $E_d^W(0)$ at the surface z = 0;

(2) The downwelling slope, $\frac{dE_d^w(0)}{dz} = \beta_d(0)$, at the surface z = 0;

(3) The upwelling irradiance $E_u^W(h) = Euh = Rb(E_{dh})$ at the bottom z = h;

(4) The upwelling slope, $\frac{dE_u^w(h)}{dz} = \beta_u(h)$, at the bottom z = h;

The general solutions for downwelling and upwelling irradiances are:

$$E_d^w(Z) = \frac{E_d^w(0)}{2}(e^{\psi z} + e^{-\psi z}) + \frac{bE_{u0} - (a+b)E_d^w(0)}{2\psi}(e^{\psi z} - e^{-\psi z}) \tag{6}$$

$$E_u^w(Z) = \frac{R_b E_{dh}}{2}[e^{\psi(h-z)} + e^{-\psi(h-z)}] + \frac{bE_{dh} - (a+b)}{2}[e^{\psi(h-z)} + e^{-\psi(h-z)}]. \tag{7}$$

Reflectance in the water is defined as the ratio of the upwelling radiation to the downwelling radiation and, as a result, is non-dimensional, always less than unity, and can be written using Equations (6) and (7) as:

$$R_w(z) = \frac{\psi R_b E_{dh}[e^{\psi(h-z)} + e^{-\psi(h-z)}] - [-bE_{dh} + (a+b)]E_{uh}[e^{\psi(h-z)} + e^{-\psi(h-z)}]}{\psi E_d^W(0)(e^{\psi z} + e^{-\psi z}) + [bE_{u0} - (a+b)E_d^W(0)](e^{\psi z} + e^{-\psi z})}. \tag{8}$$

where $E_d^W(0)$ is downwelling irradiance at the surface, E_{u0} is calculated upwelling irradiance at the surface, E_{dh} is downwelling irradiance at the bottom, E_{uh} is upwelling irradiance at the bottom, h is water depth, and R_b is the bottom reflectance.

The reflectance just below the surface can be obtained by taking the ratio of the equation of the upwelling irradiance at the surface to the downwelling irradiance on the surface, along with a substitution of Equations (2) and (3) for the appropriate boundary conditions, i.e. for boundary conditions (2) and (4) above. This allows the expression below to be algebraically determined:

$$R_w(0) = \frac{R_b\left(\frac{X^2}{4} - \frac{XYa}{2\psi} - \frac{XYb}{2\psi} + \frac{Y^2a^2}{4\psi^2} + \frac{Y^2ab}{2\psi^2} + \frac{Y^2b^2}{4\psi^2}\right) + \frac{XYb}{4\psi} - \frac{Y^2ab}{4\psi^2} - \frac{Y^2b^2}{4\psi^2}}{1 - \frac{R_bYb}{4\psi^2}(\psi X - Ya - Yb) - \frac{Y^2b^2}{4\psi^2}}. \tag{9}$$

where $X=(e^{\psi h}+e^{-\psi h})/2$, $Y=(e^{\psi h}-e^{-\psi h})/2$. Equation (9) is a function of a, b, h, and R_b all of which are assumed to be parameters for model computations, therefore, $R_W(0,\lambda)$ can be calculated (or measured by a remote sensing system), and $a(\lambda)$, $b(\lambda)$, h, and $R_b(\lambda)$ are all specified values at any one wavelength or appropriate bandwidth. This analytical expression is here used in this paper to calculate the irradiance reflectance just below the water surface. This irradiance reflectance is a measure of the relative backscattered light just below the water column. Note that it is the spectral shape of $R_W(0)$ as a function of wavelength that ultimately contains the information concerning the composition of water quality constituents in the medium. Thus, it is the parameter of interest for the optical oceanographer. To calculate the above water surface

reflectances the upwelling irradiance must be transmitted through the water surface using the internal reflectances written as:

$$R_A(0) = \frac{(1 - R_{Di})E_u^w(0) + R_D E_D + R_S E_S}{E_D + E_S}. \tag{10}$$

where R_{Di} is internal diffuse reflectance, the term $R_D E_D$ is the surface reflected skylight (skyglint), and the term $R_S E_S$ is the surface reflected sunlight (sunglint).

4.2. Case II: The non-homogeneous two-flow model with a specular irradiance (collimated irradiance), $E_s^w(z)$, is:

$$\frac{dE_d^w(z)}{dz} = -(a+b)E_d^w(z) + bE_u^w(z) + cE_s^w(z). \tag{11}$$

$$\frac{dE_u^w(z)}{dz} = (a+b)E_u^w(z) - bE_d^w(z) - cE_s^w(z). \tag{12}$$

$$\frac{dE_s^w(z)}{dz} = kE_s^w(z). \tag{13}$$

where c is the conversion coefficient and k is the beam attenuation coefficient both with units m^{-1}. Here the gain of upwelling irradiance is also due to scattering (conversion) of specular flux density. The four parameters a, b, c, and k can be assumed constant or can be calculated as functions of the sun angle and optical properties of the in-situ water taken from depth z. Similarly, a set of decoupled second order non-homogeneous irradiance equations are given as follows:

$$\frac{d^2E_d^w(z)}{dz^2} - (a^2 + 2ab)E_d^w(z) = c(k - a - 2b)E_s^w(z). \tag{14}$$

$$\frac{d^2E_u^w(z)}{dz^2} - (a^2 + 2ab)E_u^w(z) = -c(k + a + 2b)E_s^w(z). \tag{15}$$

along with a third equation:

$$\frac{dE_s^w(z)}{dz} = kE_s^w(z). \tag{16}$$

The general solutions for downwelling, upwelling, and specular irradiance are, respectively,:

$$E_d^w(Z) = \frac{\psi[m + E_d^w(0)] + [km - (a+b)E_d^w(0) + bE_{u0} + cE_s^w(0)]}{2\psi} e^{\psi z}$$
$$+ \frac{\psi[m + E_d^w(0)] - [km - (a-b)E_d^w(0) + bE_{u0} + cE_s^w(0)]}{2\psi} e^{-\psi z} - me^{kz}. \tag{17}$$

$$E_u^w(Z) = \frac{\psi e^{-\psi h}[ne^{kh} + R_b(E_{dh} + E_{sh})] + e^{-\psi h}(kne^{kh} + (a+b)E_{uh} - bE_{dh} - cE_{sh})}{2\psi} e^{\psi z}$$
$$+ \frac{\psi e^{\psi h}[ne^{kh} + R_b(E_{dh} + E_{sh})] - e^{\psi h}[kne^{kh} + (a+b)E_{uh} - bE_{dh} - cE_{sh}]}{2\psi} e^{-\psi z} - ne^{kz}. \tag{18}$$

$$E_s^w(Z) = E_s^w(0)e^{kz}. \tag{19}$$

Reflectance for this case is defined as the ratio of the upwelling irradiance to the sum of downwelling irradiance and specular irradiance, and as a result is non-dimensional, always less than unity, and can be written as:

$$R_w(z) = \frac{E_u^w(z)}{E_d^w(z) + E_s^w(z)} \qquad (20)$$

5. MODEL SIMULATION AND TESTING

Only the homogeneous model (Case I) is simulated and applied to the light propagation in the water for this paper using calculted absorption and backscatter data taken from Bostater[5]. These coefficients are used to verify the model output by: (1) observing the change in upwelling irradiance within the water column for various water and bottom types; (2) comparing it to field measured reflectance spectra taken in Delaware Bay; and (3) sensitivity analysis of the model (Case I) described for a specific set of input parameters.

5.1. Upwelling Irradiance Within a Water Column

The upwelling irradiance, $E_u^w(z)$, through the water column with changes in bottom reflectance is displayed in Figure 3. Typical values of downwelling irradiance just outside the atmosphere were taken from Valley[6] and used in calculating the downwelling irradiance for the two-flow model with a simple atmospheric correction model[7]. Figure 3 demonstrates that $E_u^w(z)$ increases in magnitude as a function of increasing bottom reflectance and also increases near the bottom similar to results from more complex models (Case II). Figure 2 demonstrates logarithmic plots of reflectance within a water column as a function of depth from the Case I two-flow model. Note the similarity of these results to previous models described by Preisendorfer[1].

5.2. Comparison of Irradiance Reflectance Spectra Measured in Delaware Bay and Two-Flow Model Results

A high resolution spectroradiometer was used by Bostater[5] to calculate the irradiance reflectance spectra and backscatter coefficients in the lower Delaware Bay. Measured diffuse attenuation and backscatter data at stations 20, 22, 24, and 26 were used to calculate the absorption coefficients for these stations. The resulting data were used in the simplified two-flow model (Case I). and the above surface irradiances were calculated, assuming a constant bottom reflectance of 0.2 across the spectrum[7].

Figure 4 is a graph of measured above surface irradiance reflectance spectra taken from Bostater[5] at four stations. Figure 5 is a graph of the model irradiance reflectance spectra for these same stations using the simplified Case I analytical model. Figures 4 and 5 have the same spectral shapes, however the reflectance magnitudes differ by a reflectance of about 0.01. A simple atmospheric extinction model[7] was used to estimate the irradiance just above the water surface. The model utilizes the diffuse and direct components of sunlight and an atmoshperic extinction function that is wavelength dependent and dependent on zenith angle.

5.3. Sensitivity Analysis of the Two-Flow Model

For this research a sensitivity analysis was conducted for the Case I solution to the two-flow equations for optically shallow water. The analytical model is simulated and different parameter values were used to assess the sensitivity results of the model[7]. Water absorption and backscatter coefficients are taken from the literature and used for testing the model. Observed results from Bukata[8] and Bostater[5] are compared to the model output to determine if the model and underlying assumptions allow estimation of reflectance signature.

The sensitivity analysis was run at four separate wavelengths 430, 490, 540, and 685 nm for each variable with a 90% change interval and then a 2% change interval in model state variables using the method described by Bostater[9,10] in

a coupled physical-bio-optical model. The model state variables were ranked according to the degree to which they influenced the reflectance output. Table 1 shows the most sensitive variables (ranked 1) and those model variables which least affected the reflectance standard run case for lower Delaware Bay water types. As indicted for this deep water case (h = 15 m), the water depth becomes less important when compared to the absorption, backscatter, and internal diffuse reflectance processes. Althrough not shown here, the result for the optically shallow case will cause water depth to become a dominant model variable affecting modeled reflectance signatures. The influence of bottom reflectance and water depth, as well as water quality parameter concentration, is shown in figures 6 through 17 and described below.

Table 1. Normalized Mean Sensitivity Values 490nm

Model Variable	Sensitivity Scale
Absorption	1.00
Internal diffuse reflectance	0.97
Backscatter	0.66
External diffuse reflectance	0.34
Ratio of skylight to sunlight	0.31
Bottom reflectance	0.24
Water depth	0.06
Zenith angle	0.03

After Lamb[7]

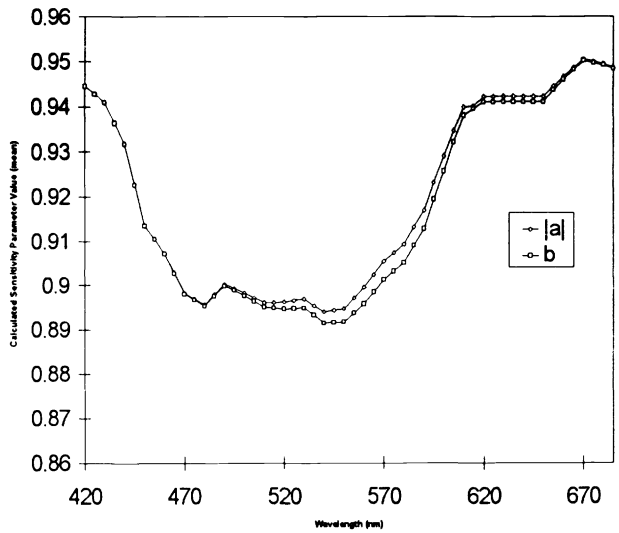

Figure 1. Plot of the mean sensitivity parameter of the backscatter coefficient and the absolute value of the mean sensitivity of the absorption coefficient using the method described by Bostater[9,10].

6. RESULTS AND DISCUSSION

The simplified Case I two-flow model used in this model evaluation study can reproduce reflectance signatures similar to those taken in the field. Figures 4 and 5 are examples of this similarity however the magnitude of the predicted reflectance signature is slightly higher in Figure 5 than the measured reflectance in Figure 4. This results are indicative of the model results before the model was calibrated. This could be due to a number of assumptions made in the model such as the distribution function being taken as equal to one. Also, if the water surface is not flat, the internal diffuse reflection coefficient increases, resulting in a sensor above the water surface measuring less upwelling radiation from a rough water surface than a flat water surface. This increase in internal reflection is due to internal surface reflections and wave focusing effects. It is also known that the Fresnel reflection increases as a function of wind speed due to the surface no longer being smooth. As the wind speed increases, the surface reflection above and below the water also increases. The version of the model presented here does not consider wind effects. It should also be noted that for small observation angles, wind speed does not have a strong effect.

The assumption that the absorption and backscatter coefficients are constant for both directions and as a function of depth may be suitable for well mixed waters. Other two-flow models such as a two-flow model developed by Ackleson and Klemas[4] and Philpot's[11] single-scattering model can be utilized to as well as differentiating between upward and downward absorption and backscatter coefficients. Philpot[11] indicates that if the upwelling attenuation is equal to the downwelling attenuation then the in water reflectance is constant with depth. However, note in Figure 2 that we show that the water reflectance can vary as a function of depth in this simplistic Case I model with upwelling and downwelling attenuation being constant in optically shallow waters..

It should be noted that the sensitivity analysis in Table 1 only applies for λ = 490 nm and standard input values specific to a mid-Atlantic coastal plain estuary. These sensitivities will change depending on the standard run used as well as the wavelengths and bandwidths chosen. For example if the water column were more shallow, the bottom reflectance sensitivity would increase relative to the water absorption and backscatter sensitivities. The model derived reflectance signatures shown in Figures 6 to 17 are model results where realistic bottom types and a shallow water (h = 3 m) body are used to model the surface water reflectance signatures. Bottom reflectance types used in the Case I model simulations reported here includes a constant value of R_b = 0.2 (where indicated) at all wavelengths or bottom reflectance signatures (368 - 1115 nm) of a white sandy bottom, a sand and sea grass mixture bottom, a bleached or dead coral reef bottom, a healthy Elk Horn coral bottom, and a pure sea grass (turtle grass) bottom. Note how different water constituents (chlorophyll-a, dissolved organic carbon-DOM, and suspended sediment or seston), water depth, and bottom types affect the simulated spectral signature. In general, the model behaves according to our scientific understanding of reflectance signatures as vividly described by Robinson[12].

7. ACKNOWLEDGMENTS

Model simulations were performed on an Indigo^2 workstation. Indirect support has been provided by Don Riordan and Ken Marcks, Silicon Graphics Inc. and K.B. Science and Engineering. Dr. William Naught, NASA, Kennedy Space Center, is acknowledged for supporting this research. Dr. R. Sullivan, Florida Tech, is thanked for his support in the development of the Marine & Environmental Optics Lab and the Remote Sensing Center at Florida Tech.

8. REFERENCES

1. R.W. Priesendorfer, *Hydrologic Optics*, Vol I-VI, 1757 pp, NOAA/ERL, Honolulu, Hawaii, 1976.
2. C.B. Bostater, Wei-Ming Ma and A.P. Lamb, "Simulating radiative transfer in aquatic systems and contrasting results from ambient environmental spectroscopy: estuarine and near coastal waters," In: Proc. 2nd Intl. Conference on Spectral Remote Sensing Research, SanDiego, CA, USACOE, 9 pp, July 1994.
3. C.D., Mobley, B. Gentili, H.R. Gordon, Z. Jin, G.W. Kattawar, A. Morel, P. Reinersmam, K. Stamnes, and R.H. Stavn, "Comparison of numerical models for computing underwater light fields," Applied Optics, 32(6), 7484-7504, 1993.
4. S.G. Ackleson and V. Klemas, "Two-Flow Simulation of the Natural Light Field Within a Canopy of Submerged Aquatic Plants", Applied Optics 25, 1129-1136, 1986.
5. C.B. Bostater, "Design of a multilevel remote sensing study of the Chesapeake Bay," NOAA Final Report #ED10008L1A7D4111, 27 pp, 1990.
6. S.L. Valley, *Handbook of geophysics and space environments*, 1.0-22.15, Air Force Cambridge Research Laboratories, 1965.
7. A.P. Lamb, Sensitivity analysis of an optical remote sensing model, Master Thesis, Florida Institute of Technology, 136 pp, 1995.
8. R.P. Bukata, J.E. Bruton and J.H. Jerome. "Use of chromaticity in remote sensing measurements of water quality," Remote Sensing of the Environment 13, 161-177, 1983.
9. C.B. Bostater, On simulating the active vertical motion of Morone saxatilis in the estuarine environment, Ph.D. Dissertation, University of Delaware, 207 pp, 1989.
10. C.B. Bostater and R. Biggs, "Simulating the vertical motion of nekton in the estuarine environment - scientific considerations and speculations," In: Understanding the Estuary: Advances in Chesapeake Bay Research. Proc. of a Conf., Baltimore, MD, 92-108, Mar, 1988.
11. W.D. Philpot, "Radiative Transfer in Stratified Waters: A Single-Scattering Approximation for Irradiance," Applied Optics 26, 4123-4132, 1987.
12. I.S. Robinson, "Satellite observations of ocean colour," Phil. Trans. Roy. Soc. London A309, 415-432, 1983.

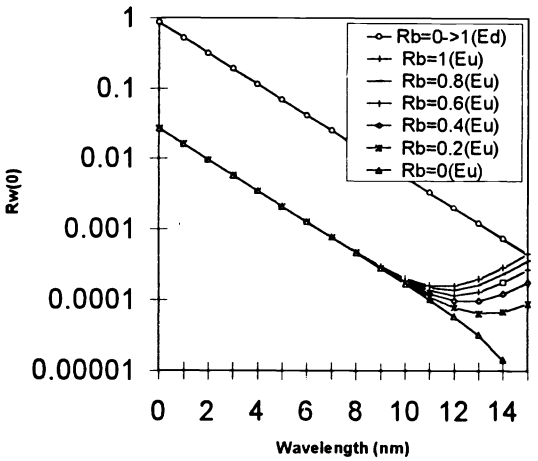

Figure 2. Logarithmic plots of downwelling and upwelling irradiance within a water column as a function of depth from the Case I two flow model. The profiles are shown for different bottom reflectances using λ=430 nm and data from station 26 (h=15m) reported by Bostater[5] and Lamb[7].

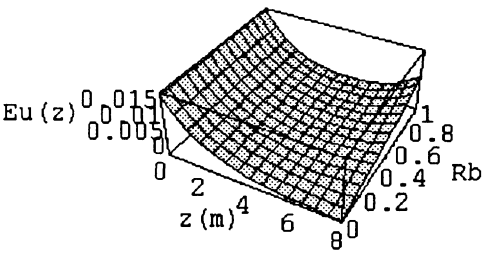

Figure 3. Graph demonstrating the phenomenon of increased upwelling irradiance (W/m^2/nm) near the bottom for a typical coastal water body at a wavelength of 430 nm. The bottom reflectance is varied from 0 to 1 and the water depth is 8 m. After Lamb[7].

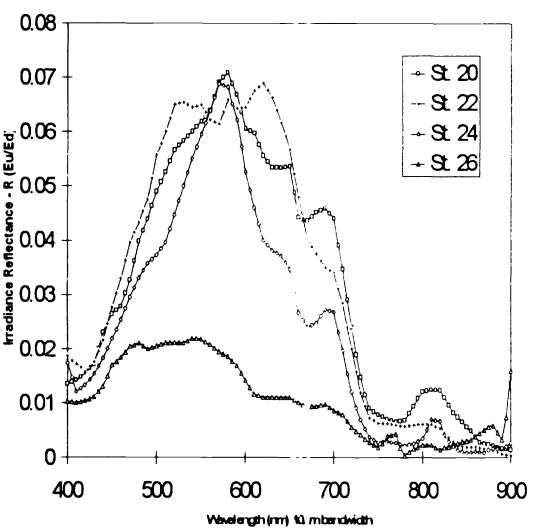

Figure 4. Measured above water irradiance reflectance spectra from Bostater[5]. Note higher reflectance values with increasing water turbidity as one goes up estuary (station 20).

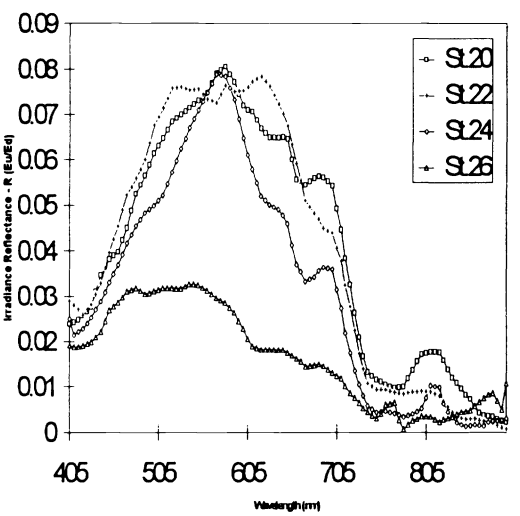

Figure 5. Model derived (Case I) two-flow model output of the above water irradiance reflectance spectra, Lamb[7]. Assumed constant bottom reflectance=0.2, zenith angle=20 degrees, and h=15 m. Note the similar spectral shapes to Figure 4.

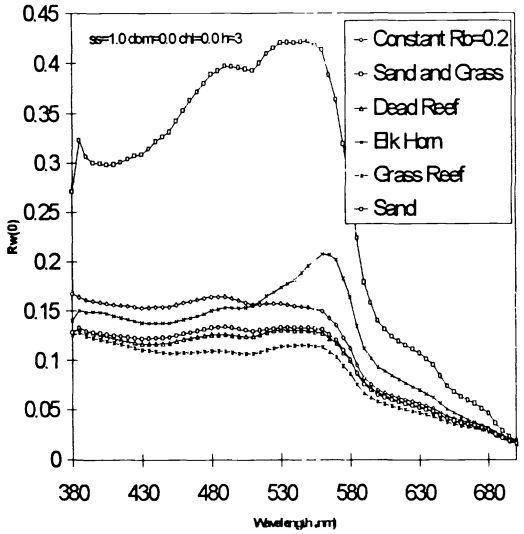

Figure 6. Model derived subsurface irradiance reflectance spectra for various bottom reflectance Rb(λ) spectra with suspended matter = 1 mg L^{-1} (h=3 m). Concentrations of dissolved organic matter and chlorophyll are zero.

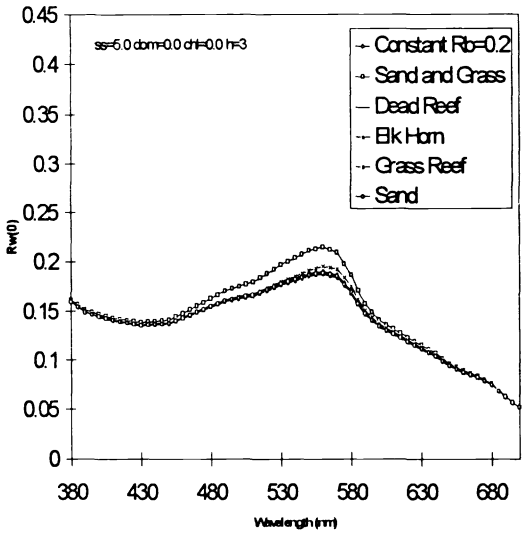

Figure 7. Model derived subsurface irradiance reflectance spectra for various bottom reflectance Rb(λ) spectra with suspended matter = 5 mg L^{-1} (h=3 m). Concentrations of dissolved organic matter and chlorophyll are zero.

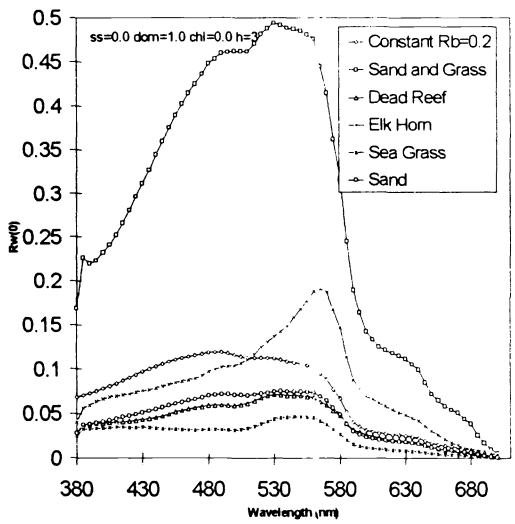

Figure 8. Model derived subsurface irradiance reflectance spectra for various bottom reflectance Rb(λ) spectra with dissolved organic matter (carbon) =1.0 mg(C) L^{-1} (h=3 m). Concentrations of suspended matter and chlorophyll are zero.

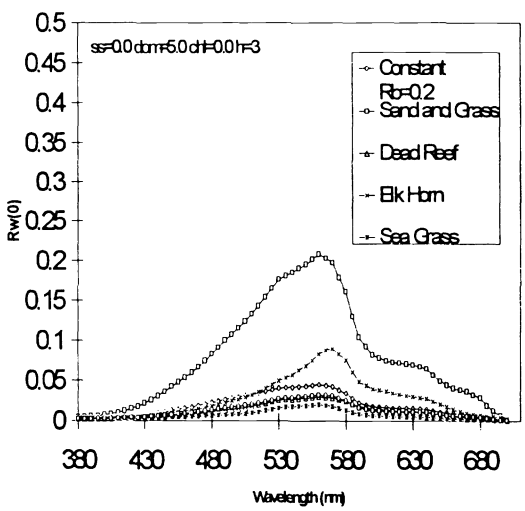

Figure 9. Model derived subsurface irradiance reflectance spectra for various bottom reflectance Rb(λ) spectra with dissolved organic matter (carbon) =5.0 mg(C) L^{-1} (h=3 m). Concentrations of suspended matter and chlorophyll are zero.

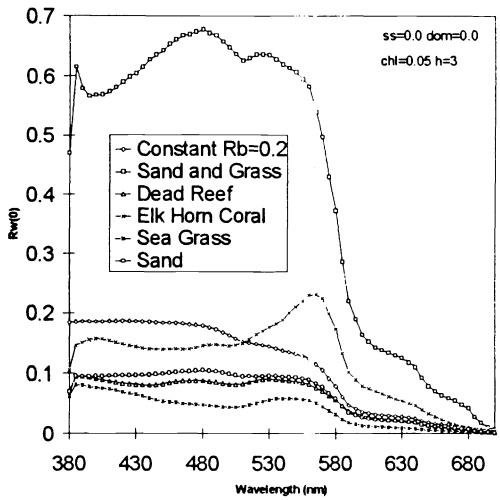

Figure 10. Model derived subsurface irradiance reflectance spectra for different bottom reflectance spectra and a chlorophyll concentration of 0.05 $\mu g\ L^{-1}$ (h=3 m). Concentrations of dissolved organic matter and suspended matter are zero.

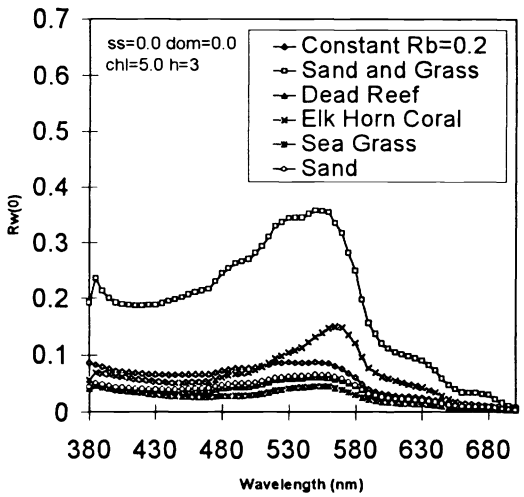

Figure 11. Model derived subsurface irradiance reflectance spectra for different bottom reflectance spectra and a chlorophyll concentration of 5.0 $\mu g\ L^{-1}$ (h=3 m). Concentrations of dissolved organic matter and suspended matter are zero.

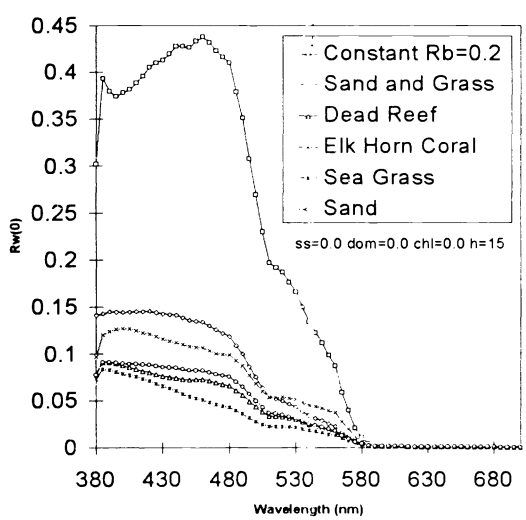

Figure 12. Model derived subsurface irradiance reflectance spectra for different bottom reflectance spectra and chlorophyll-a=0.05 $\mu g\ L^{-1}$ (h=15 m). Concentrations of dissolved organic matter and suspended matter are zero.

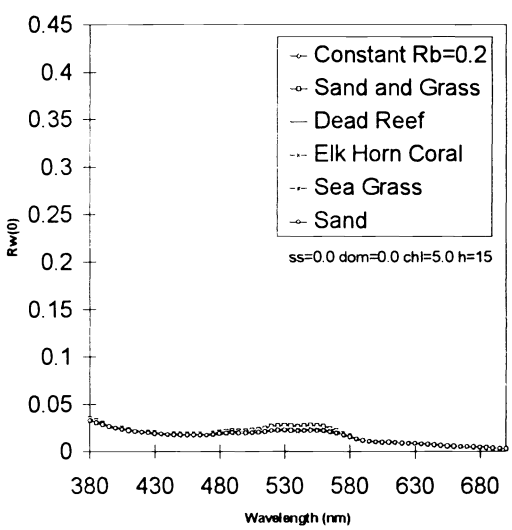

Figure 13. Model derived subsurface irradiance reflectance spectra or different bottom reflectance spectra and chlorophyll-a=5.0 $\mu g\ L^{-1}$ (h=15 m). Concentrations of dissolved organic matter and suspended matter are zero.

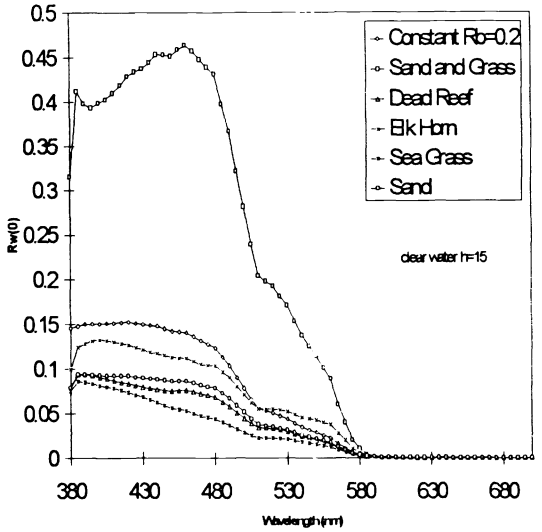

Figure 14. Model derived subsurface irradiance reflectance spectra for clear water using various bottom reflectance Rb(λ) spectra (h=15m). Concentrations of chlorophyll, suspended matter, and humic substances are zero.

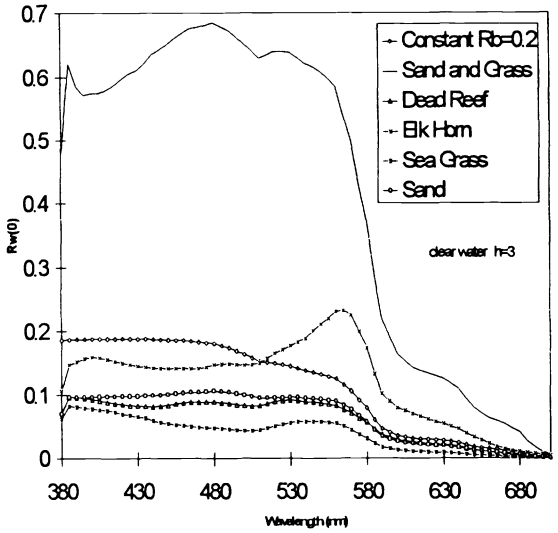

Figure 15. Model derived subsurface irradiance reflectance spectra for clear water using various bottom reflectance Rb(λ) spectra (h=3m). Concentrations of chlorophyll, suspended matter, and humic substances are zero.

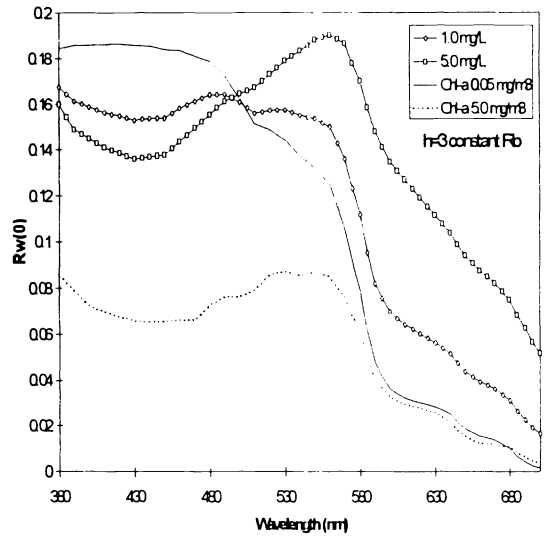

Figure 16. Model derived subsurface irradiance spectra for suspended matter concentrations of 1.0 and 5.0 mg L^{-1}, concentrations of 0.05 and and 5.0 μg L^{-1} for chlorophyll, and a constant bottom reflectance of 0.2 (h=3m). Concentration of dissolved organic matter is zero. ***Note the characteristic hinge point phenomena.***

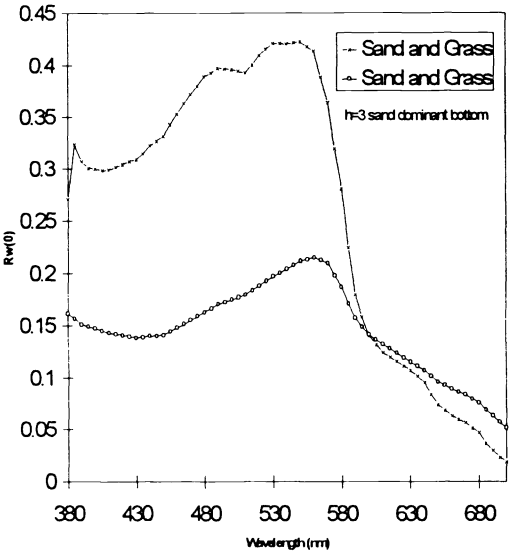

Figure 17. Model derived subsurface irradiance reflectance spectra with suspended matter concentrations of 1.0 and 5.0 mg L^{-1} with a sand dominant bottom reflectance spectrum (h=3m). Concentrations of chlorophyll and dissolved organic matter are zero.